The evolution of the seasonal ice mass balance buoy

Cameron J. Planck[a,*], James Whitlock[a], Chris Polashenski[a,b], Donald Perovich[a]

[a] Thayer School of Engineering at Dartmouth College, 14 Engineering Drive, Hanover, NH 03755, United States
[b] Cold Regions Research and Engineering Laboratory, Alaska Projects Office, Building 4070 9th Street, Fort Wainwright, AK 99703, United States

ARTICLE INFO

ABSTRACT

Arctic sea ice plays a crucial role in the global climate system, acting as both an indicator and an amplifier of climate change. Sea ice mass balance, which is simply the net difference between ice grown and ice melted, is an important parameter that can connect changes in ice thickness to environmental forcings. Opportunities for long-term observations of sea ice mass balance have been greatly expanded by the use of autonomous ice mass balance buoys, which are able to resolve changes to local ice mass balance by measuring time series of snow depth and ice surface and bottom position. This paper presents the design for a newly improved Seasonal Ice Mass Balance buoy (referred to as SIMB-3) that was created to enhance the ability to monitor mass balance with design features that maximize reliability and survivability, reduce installation difficultly, and reduce cost. Operational advancements were also made to make the buoy easy to manufacture, ship worldwide, and assemble in the cold. A custom low-cost datalogger-controller was developed to operate the mass balance sensor package while allowing future expandability for use with non-standard instruments. Several test deployments were conducted in 2018, and the instrument demonstrated ability to successfully collect mass balance data in seasonal sea ice. Results from one of these test deployments in the Beaufort Sea during April 2018, are presented and discussed.

1. Introduction

Arctic sea ice has experienced a significant decline over the past 30 years. Satellite derived estimates of sea ice extent have shown a downward trend in the September minima of 13.2% decade^{-1} when compared to the 1981–2010 average (Richter-Menge et al., 2018). Accompanying large reductions in sea ice extent are large reductions in thickness, and a general replacement of multi-year ice with first year ice. From 2003 to 2008, the Arctic-wide percentage of first year ice surpassed the percentage of multiyear ice, shifting from 38% first year ice by volume in 2003 to 68% in 2008. (Kwok et al., 2009). The downward trend in summer ice extent and thickness has been attributed to a range of interconnected processes, including ice-albedo feedback (Perovich and Polashenski, 2012), cloud and wind influence (Kay and Gettelman, 2009), and increasing Arctic air temperatures (Stroeve et al., 2012). While the changes occurring to the Arctic sea ice are well documented, the atmospheric and oceanic forcings driving the change are not fully understood (Carmack and Melling, 2011). One method for studying the net effect of these forcings is by monitoring the thermodynamic sea ice mass balance, which is the difference between ice growth and ice melt over a period of time. Because sea ice exists at the boundary of ocean and atmosphere, its mass is controlled by energy fluxes at this interface. If there is a net cooling over time, the ice will thicken; if there is a net warming over time, ice will thin. The timing and location of melt and growth (e.g. surface vs bottom melting) can be used to attribute observed changes to specific environmental forcings (e.g. atmospheric vs. oceanic heat flux) (Light et al., 2011; Perovich et al., 2008).

Time series observations of sea ice thickness are difficult to obtain across all scales. Thickness estimations have been made through a variety of means, including submarine mounted upward looking sonar (Rothrock et al., 2008), anchored upward looking sonar (Krishfield et al., 2014), electromagnetic induction sensors, and airborne and satellite based LIDAR and radar altimeters (Kwok et al., 2009; Kwok and Cunningham, 2015; Laxon et al., 2013), but vary significantly in accuracy and spatial resolution (Lindsay and Schweiger, 2015). Moreover, all of these remote sensing technologies lack the ability to delineate between surface and bottom melting, a feature that is crucial for attributing changes in mass balance to atmospheric or oceanic forcing.

In situ observations of local thermodynamic ice mass balance have been made as part of manned field campaigns as well (Perovich, 2003; Untersteiner, 1961), but the high costs and logistical difficulties of sustaining manned operations on the drifting sea ice cover have limited measurements by this method in both space and time. The need for

---

* Corresponding author.
  E-mail address: Cameron.j.planck.th@dartmouth.edu (C.J. Planck).

more frequent and higher density sea ice mass balance observations thus motivated the development and deployment of autonomous instruments, generally referred to as Ice Mass Balance Buoys (IMB's) (Jackson et al., 2013; Polashenski et al., 2011; Richter-Menge et al., 2006). These instruments measure ice surface and bottom position over time, and are used to determine changes to local thermodynamic mass balance. Here we discuss an improved IMB, which has been comprehensively engineered to be a reliable, affordable, and accurate system for measuring thermodynamic seasonal ice mass balance.

1.1. Background: the ice mass balance buoy

Since 1993, Ice Mass Balance Buoys developed at the US Army Cold Regions Research and Engineering Laboratory in Hanover, New Hampshire, USA, have been deployed as a part of a variety of observational efforts. Programs include the North Pole Environmental Observatory (NPEO) (Morison et al., 2002), the International Polar Year (IPY), the Beaufort Gyre Exploration Project, and the Arctic Observing Network (AON). IMB's autonomously collect a suite of in situ measurements, including ice surface and bottom position, ice drift, meteorological data, and snow-ice-ocean temperature profiles (Richter-Menge et al., 2006). The standard instrument package consists of a downward-facing acoustic rangefinder positioned above the ice measuring surface position, an upward-facing acoustic rangefinder positioned underneath the ice measuring bottom position, a vertical temperature string through the air-snow-ice-ocean interface, and air temperature and pressure sensors (Fig. 1,a). All sensors communicate through a satellite-connected electronics package which transmits data at user selected intervals, typically every 1–4 h.

As seen in Fig. 1,a, the IMB data controller housing is non-floating and relies on the ice for mechanical support, an attribute that limits the IMB when collecting data in seasonal ice. This limitation was addressed

in 2011 with the advent of the Seasonal Ice Mass Balance buoy (SIMB-1). The SIMB-1 is equipped with the same sensor package as the IMB, but is enclosed in a cylindrical, upward-floating buoy hull (Fig. 1,b) (Polashenski et al., 2011). The SIMB-1 was designed to measure the ice without disturbing it, and its ability to float makes it survivable in thin, seasonal ice. This feature permits data collection farther into the melt season, which is a time of significant scientific interest that was largely lacking in observations.

Since 2011, several SIMB-1 prototypes have been deployed, and the platform demonstrated the ability to measure mass balance in seasonal sea ice. This success was followed with the creation of SIMB-2, which was largely the same as the SIMB-1, but built with a slightly different electronics package and smaller diameter hull. Only a handful of SIMB-2's were ever produced, and the bulk of the existing SIMB data was gathered using SIMB-1's. Both SIMB-1 and SIMB-2 were prototype-level devices with very high part costs and extensive assembly labor requirements. These prototype platforms successfully validated the SIMB concept however, and motivated a full development process with the overarching goals of i.) ensuring reliability and maximizing survivability; ii.) simplifying construction; iii.) reducing instrument size and weight; iv.) reducing cost; and v.) reducing installation complexity. Achieving these goals is key to enabling more science by i.) reducing instrument failures; ii.) reducing deployment complexity and specialized labor requirements; and iii.) allowing more SIMB's to be produced at lower cost. This paper outlines the design of the latest SIMB platform, which was created with these goals as priority. The newly designed SIMB will hereafter be referred to as SIMB-3.

2. Design methods

Experience has demonstrated that many criteria must be considered for an autonomous system to be effective at producing data in the
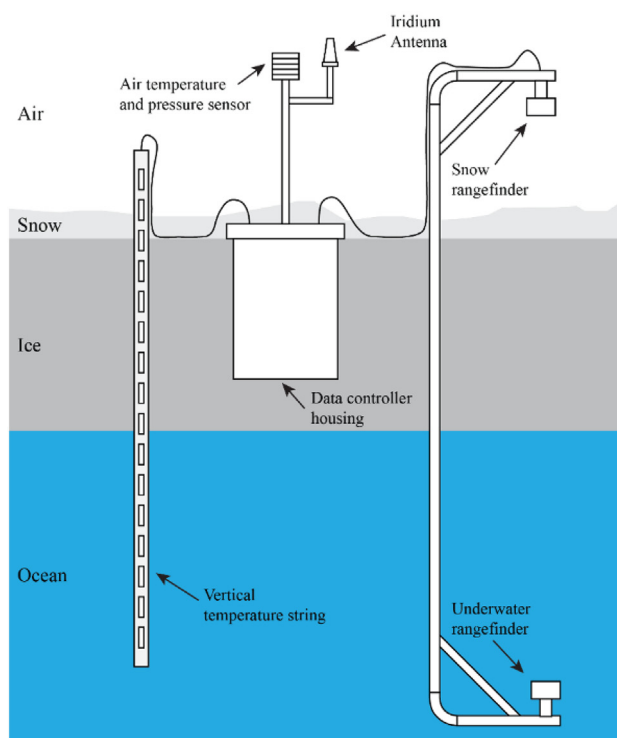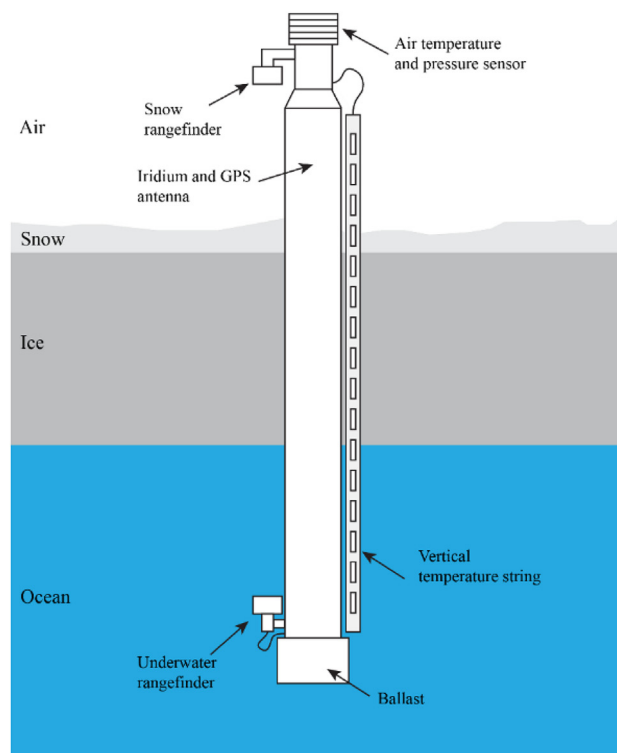
Fig. 1. (a) Ice Mass Balance Buoy (IMB) schematic. The instrument is equipped with two ice facing acoustic rangefinders, a vertical temeperature string, and air temperature and pressure sensors. All sensors are connected to a non-floating satellite connected transmission package. (b) Seasonal Ice Mass Balance Buoy (SIMB-1). The SIMB-1 instrument has the same sensor package as the IMB, but enclosed in spar-type buoy hull that is frozen into the ice.

Arctic. While the device must be able to collect the required data, other attributes such as survivability, instrument size and shipping weight, data format, data transmission interval, deployment ease, assembly time, and assembly complexity also influence device efficacy over the instrumentation lifecycle (Massonnet and Jahn, 2012). Additionally, the sea ice is generally remote, making revisiting deployment sites logistically difficult and often cost prohibitive. These limitations underscore the need for highly controlled manufacturing and quality control processes to maximize reliability.

To structure the SIMB-3 redesign, a formal Quality Functional Deployment (QFD) design process was undertaken (Hauser et al., 2010). Stakeholders were identified and surveyed for their opinions and desired improvements for SIMB-3. The survey results were then translated into engineering requirements and used in a House of Quality (HOQ) matrix to prioritize design criteria. The HOQ process output a set of quantitative, ranked, requirements that drove the detailed design phase and established the benchmarks used to evaluate performance during testing.

2.1. Stakeholder identification

A stakeholder was defined as any person who interacts with the physical SIMB-3 instrument or the data it produces, at any point in time. This includes persons who use the data for science, as well as persons involved in the production, transportation, or deployment processes of SIMB-3.

To demarcate interests, stakeholders were broken into two categories: primary and.

secondary. A primary stakeholder is the customer, typically a data-driven investigator or.

monitoring agency. Their requirements drove the SIMB-3 design from a scientific point of view, such as requiring the SIMB-3 to measure ice thickness through a melt season, or requiring it to be expandable for use with non-standard instruments. A secondary stakeholder is any person involved with production or operation of SIMB-3. Secondary stakeholders drove the SIMB-3 design from a practical point of view. Their interests informed design features related to the successful implementation of SIMB-3, such as manufacturability, or ease of transportation. Table 1 lists the stakeholders identified and justification for their inclusion.

2.2. Stakeholder surveys

Roughly one dozen people familiar with the (S)IMB project were selected by the authors as primary and secondary stakeholders. The people chosen all had past experience with (S)IMB's, and equally represent the categories listed in Table 1. Each stakeholder was administered a survey where they were instructed to list and rank the qualitative criteria they consider most important to the SIMB-3 design. The results from this survey were combined by the authors and used to derive a set of 16 design features that *qualitatively* define the necessary

functions of SIMB-3. These requirements are referred to as stakeholder requirements (SR's), and are listed in Table 2. It is important to note that this process was intended to outline desired improvements to the existing SIMB platform, not to reinvent a device to autonomously measure mass balance.

2.3. Engineering requirements

The stakeholder requirements listed in Table 2 were mapped to a set of quantifiable engineering requirements (ER's) by assigning one or more measurable attributes to each stakeholder requirement. Table 3 lists the SIMB-3 engineering requirements and the stakeholder requirements they address. Each stakeholder requirement in Table 2 was represented by at least one engineering requirement.

2.4. House of quality

A House of Quality matrix was constructed by the authors to correlate stakeholder requirements to engineering requirements. This process was used to highlight and prioritize contradictory stakeholder requirements, e.g. being lightweight and being stable. Rankings from the stakeholder surveys were used to weight the stakeholder requirements, and correlation coefficients of either 1 (no correlation), 3 (moderate correlation), 6 (high correlation), or 9 (direct correlation) were assigned to each of the engineering requirements to weight their relationship to each stakeholder requirement. The matrix then scored the engineering requirements based on the number, correlation, and weight of stakeholder requirements influenced. Target values and tolerances were then assigned to each of the engineering requirements to provide a quantitative metric to benchmark design solutions against. The output from this process was an ordered rank of engineering requirements that, when met, will produce a design which optimally satisfies the requirements of the stakeholders. The ranked output from this process is given in the right-most column of Table 3, and the design solutions corresponding to each engineering requirement are presented in the following section. The engineering requirements addressed by the design solutions are indicated as "[ER#]", where "#" is the engineering requirement number.

3. Technical description

3.1. Exterior design

The SIMB-3 is a 4.87 m long, 11.7 cm diameter cylindrical, unmoored spar-type buoy. The length was determined by calculating the necessary buoyancy force for stable floatation and required rangefinder offset for measuring ice up to 3 m in thickness [ER1]. A tunable and detachable ballast was included to maintain a positive righting moment while permitting adjustment of the floatation height for additional instrument payload capacity [ER6], (Fig. 2,j). The standard ballast has a mass of 10 kg to give the snow rangefinder a 1.2 m offset from the ice

Table 1
SIMB-3 stakeholders. Stakeholders have been broken into two categories, primary and secondary.

	Identified stakeholders	Justification
Primary	Lead scientist	The lead scientist is the principal stakeholder and funding source for the project.
	Collaborating scientists	Collaborators use the data and the SIMB-3 platform for a variety of purposes. Input from collaborating scientists helped inform the format, accuracy, and precision of the data reported.
Secondary	Deployment team	The deployment team is responsible for successful installation of the SIMB-3 into the ice. This includes the transport crew (e.g. pilot, loadmaster), the assembly team, and the installer and buoy operator.
	Production team	The production team is responsible for creating SIMB-3 from raw materials. This includes sourcing and purchasing all parts, and manufacturing the buoy.
	Shipper	The shipper is responsible for shipping the buoy to the deployment staging area. Their job is influenced by the size and weight of the buoy package.
	Data archiver	The data archiver is responsible for receiving the raw data from SIMB-3, doing quality control on it, and publishing it in a designated data archive.

Table 2

Requirements for the SIMB3 design as determined from stakeholder surveys.

SIMB3 will…	Lead scientist	Collaborating scientists	Deployment team	Production team	Shipper	Data technician
Collect the required data accurately	X	X		X		X
Operate as designed	X		X			
Be easily transported to the deployment site			X		X	
Blend in with the Arctic environment	X	X				
Float upright and stable in open water	X	X	X			
Have minimum power consumption	X	X				
Operate well in extremely cold environments	X	X	X			
Be quickly installed			X			
be lightweight			X	X	X	
Be quick to manufacture				X		
Minimize cost	X		X	X		
Be durable	X	X	X		X	
Operate through two melt seasons	X	X				
Be free of hazardous materials			X	X	X	
Be expandable for use with other instruments		X				
Have easily accessible data in usable format		X				X

Table 3

Engineering requirements, corresponding stakeholder requirements (SR's), and ranking. The "SR Addressed" column indicates the stakeholder requirements that each engineering requirement quantitatively addresses.

ER #	Engineering requirements (units)	SR addressed	Ranking
1	Buoy will determine surface and bottom ice position and snow depth, air pressure and temperature, vertical temperature profile, and GPS location data (y/n)	1,6,7,8,11,12,13,14,15,16	1
2	Missed or bad transmission in 30 day period (#)	1,2,5,6,7,12,13,15,16	2
16	Battery capacity (Amp Hours)	1,2,5,7,10,12,14,15,16	3
8	Minimum operating temperature of components (deg C)	1,2,8,12,13,14,15,16	4
17	Number of transmissions per day (#)	1,2,5,7,12,15	5
9	Time to install (minutes)	8,9,10,12	6
5	Distance between center of gravity and center of buoyancy (cm)	5,6,13,14,16	7
10	Total weight (kg)	3,5,6,9,10,11,12	8
19	Precision of transmitted values (#)	1,5,12,16	9
15	Installed visible profile (sq-cm)	4,13,14	10
6	Additional instrument payload capacity (kg)	1,2,5,6,10,14	11
11	Number of individual components (#)	7,9,10,11,12,13,14	12
4	Exterior color of buoy (color)	2,4,14,16	12
12	Total cost of components (USD)	8,12,13	14
13	Number of production labor hours (#)	9,10,11,12	15
14	Total weight as shipped (kg)	3,5,6,9,10,12,13	16
18	Shipping cost increase due to hazardous materials (USD)	3,12	17
7	Distance from freeboard to top rangefinder (cm)	2,6,10	18
3	Maximum compacted length (m)	2,9	19

surface at freeze-in. The hull is constructed from 4 in. nominal inside diameter cellular core ABS plumbing pipe that is coated in a white Vinyl Guard heat shrink wrap [ER4], and when installed, protrudes 1.5 m above the ice [ER7, ER15]. Cellular core ABS pipe was used for its low thermal conductivity and minimal weight when compared to the solid core PVC of previous generation buoys [ER10]. The reduction in weight and buoyancy force gained by using ABS enabled the buoy length to be shortened by 1.5 m when compared to the solid core PVC hull of previous buoys. [ER14]. This reduction in length enabled SIMB-3 to meet maximum shipping length requirements while only decoupling into two sections [ER3], simplifying deployment and manufacturing [ER11, ER13]. Fig. 2 is a schematic of the buoy.

At the top and bottom of the buoy are two ice-facing acoustic rangefinders mounted on computer numerical controlled (CNC) machined aluminum mounts (Fig. 2,c,d). This mounting configuration ensures the rangefinders remain firmly attached to the buoy hull while still allowing deployment through a 25 cm (10 in.) diameter hole [ER9]. The mounts are machined with a 6 degree outward facing bevel to direct the sonic range-finding pulse away from the buoy and reduce the possibility of the rangefinder receiving signals echoing off of the buoy hull. The upper and lower sections of the buoy are coupled together axially in the field using a 30 cm long cylindrical custom machined PVC interior coupling (Fig. 2,a,b,h). The electrical connection between top and

bottom halves is made via a pre-installed 15-conductor retractable coil cable. There are no electrical connections made during field assembly [ER9]. Once coupled, the buoy is secured together using an aluminum pin and retaining clip (Fig. 2,i). The digital temperature chain is then fastened at the end with a spring to keep the chain taut (Fig. 2,e).

3.2. Interior design

The battery, antenna, and embedded control electronics are located inside the buoy (Fig. 2,k,l). At the top of the upper section is the control board, which features a magnetic reed switch for powering the buoy, an SD card slot, and a micro USB port for programming (Fig. 2,g). The main electronics package is located at the bottom of the upper section, and consists of an Iridium satellite modem, GPS, and microprocessor attached to a custom designed main board. The battery is located at the bottom of the lower section to maximize stability [ER5]. The buoy electronics package will be discussed in greater detail in the next section.

Approximately 75% of the interior mechanical components of SIMB-3 are 3D printed in ABS or PLA plastic using a fused filament fabrication process. The use of 3D printing for manufacturing reduced fabrication labor costs by approximately 80% relative to previous generation buoys [ER12, ER13]. Additionally, the design flexibility allowed with 3D
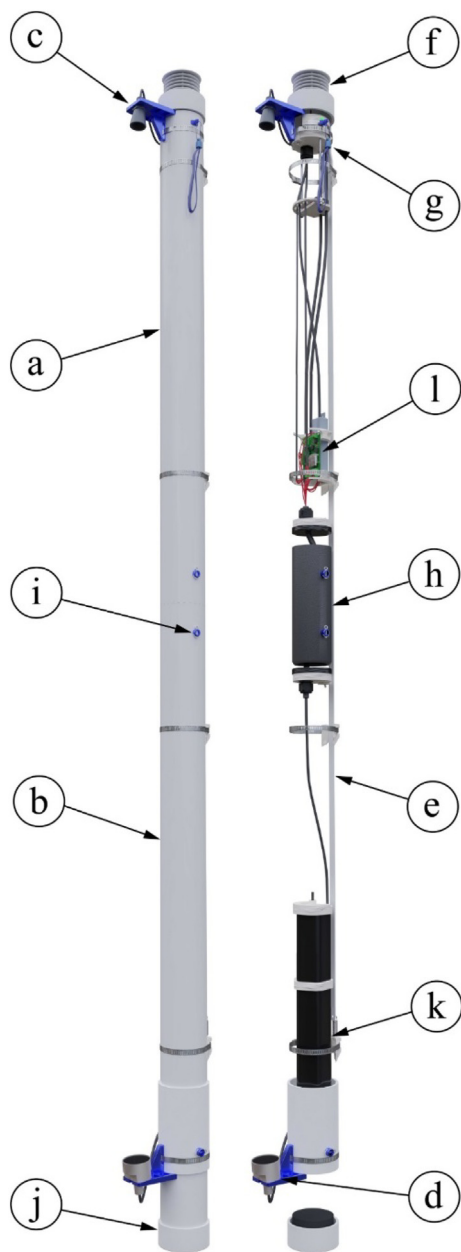
Fig. 2. Exterior schematic of SIMB-3. a: upper section, b: lower section, c: snow rangefinder, d: underwater rangefinder, e: digital temperature string, f: air temperature and pressure sensors, g: magnetic on/off switch and control board, h: coupling, i: coupling pin, j: removable ballast, k: battery, l: datalogger assembly.

printing permitted creative approaches to component design to allow for efficient assembly and reduced weight [ER10, ER11]. All 3D printed parts were impact and crush tested in a cold room at −20 °C during the prototype phases to ensure cold temperature reliability [ER8].

3.3. Electronics and sensor package

The SIMB-3 instrument package was designed to autonomously measure and report snow depth, ice thickness, vertical temperature profile, GPS location, air temperature, and barometric pressure. After buoy freeze-in, the two ice-facing acoustic rangefinders measure the distance to the air/snow interface from above and the ice/water interface from below, allowing determination of snow depth and ice thickness. Running along the vertical length of the buoy is a 3.85 m long digital temperature chain (DTC) that measures temperature in 2 cm intervals through the air, snow, ice, and into the ocean. Barometric pressure and air temperature sensors are located in the solar shield at the top of the upper section (Fig. 2,f). The buoy is powered by a custom 18 V, 1620 Wh alkaline battery pack that consists of 60 D-Cell batteries arranged in 5 columns each of 12 batteries in series [ER18]. This battery gives SIMB-3 an effective lifespan of 2 years once deployed [ER16]. The instrument names, descriptions, accuracies, reported precisions, and nominal costs (at the time of writing) of the SIMB-3 instruments are given in Table 4. Instruments were chosen by considering their precision, cost, weight, and commercial availability [ER19].

3.4. Datalogger

A custom datalogger was created for SIMB-3 to reduce cost and simplify assembly. The datalogger is built around the ATSAMD21G18 microcontroller (Microchip, 2018) which was chosen for its wide use in the hobbyist market and substantial open-source code base. The ATSAMD21G18 natively supports UART/USART, SPI, I^{2}C, and a 12-bit ADC communication standards, and additional hardware was added to support RS-422 and the Maxim One-Wire protocols. For location tracking, an MTK3339 GPS module was added, and data transmission is accomplished via an Iridium 9603 N modem. Buoy tilt and orientation tracking is possible via a board mounted Bosch BNO055 combination gyroscope, accelerometer, and magnetometer. Lastly, a Freetronics 5v external watchdog timer was included to ensure long-term reliability [ER2]. Every minute, the datalogger "pets" the watchdog timer, resetting it. If the datalogger fails to pet the watchdog timer within a 5 min window, the timer will activate the microcontroller reset line and reboot the system.

Power management for the SIMB-3 is also handled by the datalogger. The 18 V battery supply is stepped down to 12 V, 5 V and 3.3 V for use throughout the system. The 5 V and 3.3 V supplies use LMZ12003 3 amp SIMPLE SWITCHER® power modules. The 12 V supply uses a MIC29201-12WU low dropout fixed voltage regulator with logic level controlled electronic shutdown features. These devices allow for a compact and simple power supply where the 5 V and 12 V supplies are controlled by the ATSAMD21G18 microcontroller.

The datalogger is fully customized for the SIMB-3 but maintains adaptability for use with other battery-powered autonomous systems. Serial, SPI, and I^{2}C communication protocols are supported through separate auxiliary analog and digital I/O ports. Manufacturing of the datalogger is accomplished via low-volume printed circuit board (PCB) prototyping services with a total unit cost of $530 including the Iridium modem and combined GPS/Iridium antenna. Fig. 3 shows a picture of the board prior to component installation.
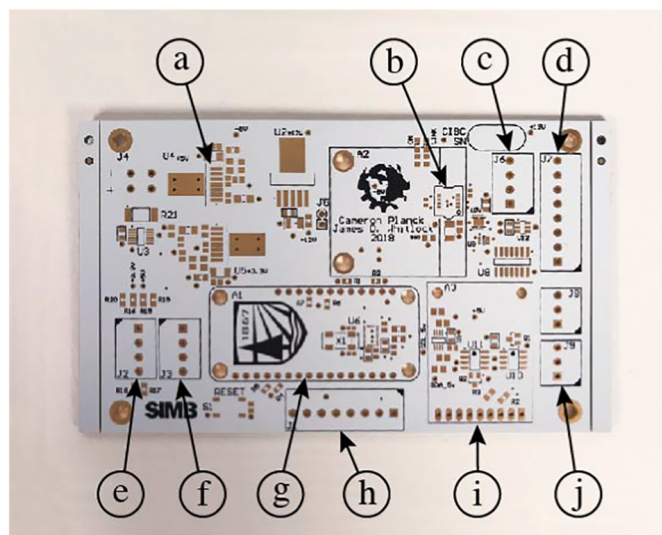
Table 4
SIMB-3 instruments, descriptions, accuracies, reported precisions, and cost.

Instrument	Description	Accuracy	Reported precision	Cost (USD)
Maxbotix MB7374	Downward looking snow rangefinder	± 0.001 m	0.001 m	$230
Airmar EchoRange+	Upward looking underwater rangefinder	± 0.01 m	0.01 m	$558
Bruncin 3.85 m DTC	High resolution digital temperature chain	± 0.25 °C	0.125 °C	$2568
DS18B20	Air temperature sensor	± 0.5 °C	0.0625 °C	$10
Bosch BME280	Barometric pressure sensor	± 0.01 mbar	0.1 mbar	$20
MTK3339 GPS	GPS module for position tracking	3 m	~0.1 m	$40

Fig. 3. SIMB-3 Main Board. a: power supply section, b: Iridium 9603 N connector, c: snow rangefinder input, d: underwater rangefinder input, e: barometer input, f: auxiliary analog input, g: ATSAMD21G18, h: digital temperature string input, i: GPS input, j: air temperature input.

Fig. 4. The February deployment of the SIMB-3 prototype in a freshwater pond near Hanover, NH. The prototype deployment validated the SIMB3's ability to accomplish the operational and scientific design requirements.
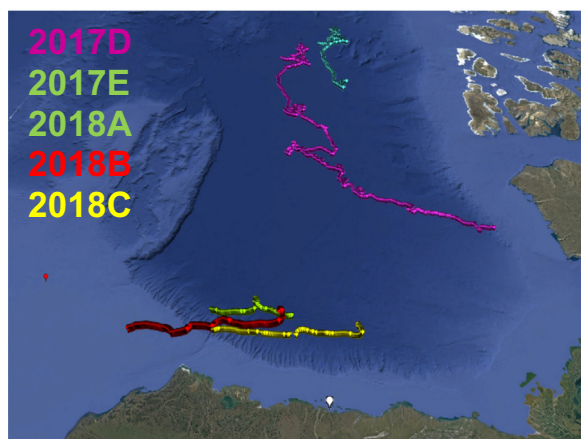
3.5. Data package and communication

On user defined intervals, usually every hour, the sensor readings and GPS location are collected and transmitted via the Iridium Short Burst Data (SBD) satellite messaging service to a remote server [ER17]. Prior to transmission, the data package is compressed into a 275-byte message to minimize data package size and reduce transmission cost. Every hour, the remote server retrieves the messages, decompresses them, and generates a human-readable spreadsheet that is web-hosted for viewing by anyone with an internet connection. Data can be viewed in semi-real time at http://imb-crrel-dartmouth.org.

3.6. Operational considerations

A defining feature of the SIMB-3 design process was the inclusion of the deployment and production teams as stakeholders. The impact of this is consideration of buoy performance from manufacturing and installation points of view in addition to scientific performance.

A central slip fit coupling and ballast attachment allows the buoy to be field assembled in four steps with no required tools, simplifying deployment [ER9]. Powering the buoy is a simple one step operation that is completed by removing an externally located key which holds a magnetically operated reed switch open (Fig. 2,g). SIMB-3 weighs 34 kg, making it approximately 50% lighter than the SIMB-1/SIMB-2 and allowing for one-person field assembly and deployment [ER10]. Even with reduced weight, buoy stability is maintained by locating the battery and a 10 kg lead ballast at the lowest possible position in the buoy hull. The battery and ballast make up 55% of the total buoy weight, and locating them at the bottom of the lower section places the center of gravity far below the buoy center of buoyancy, ensuring a positive righting moment and upright orientation during freeze-in. SIMB-3 deployment takes less than one hour, and can be done by personal without specialized training. Lastly, a custom shipping crate was designed that breaks down into a carry case during deployment. The carry case allows for easy and lightweight transport from the staging area to deployment site, and is designed to fit on a snow machine sled or in a helicopter. The box is made from heat-treated wood to abide by importation/exportation regulations of countries worldwide [ER18].

4. Test programs and discussion

A prototype SIMB-3 was constructed in January of 2017, and in February was deployed for testing in a local frozen freshwater pond near Hanover, New Hampshire (Fig. 4). The buoy was hand carried
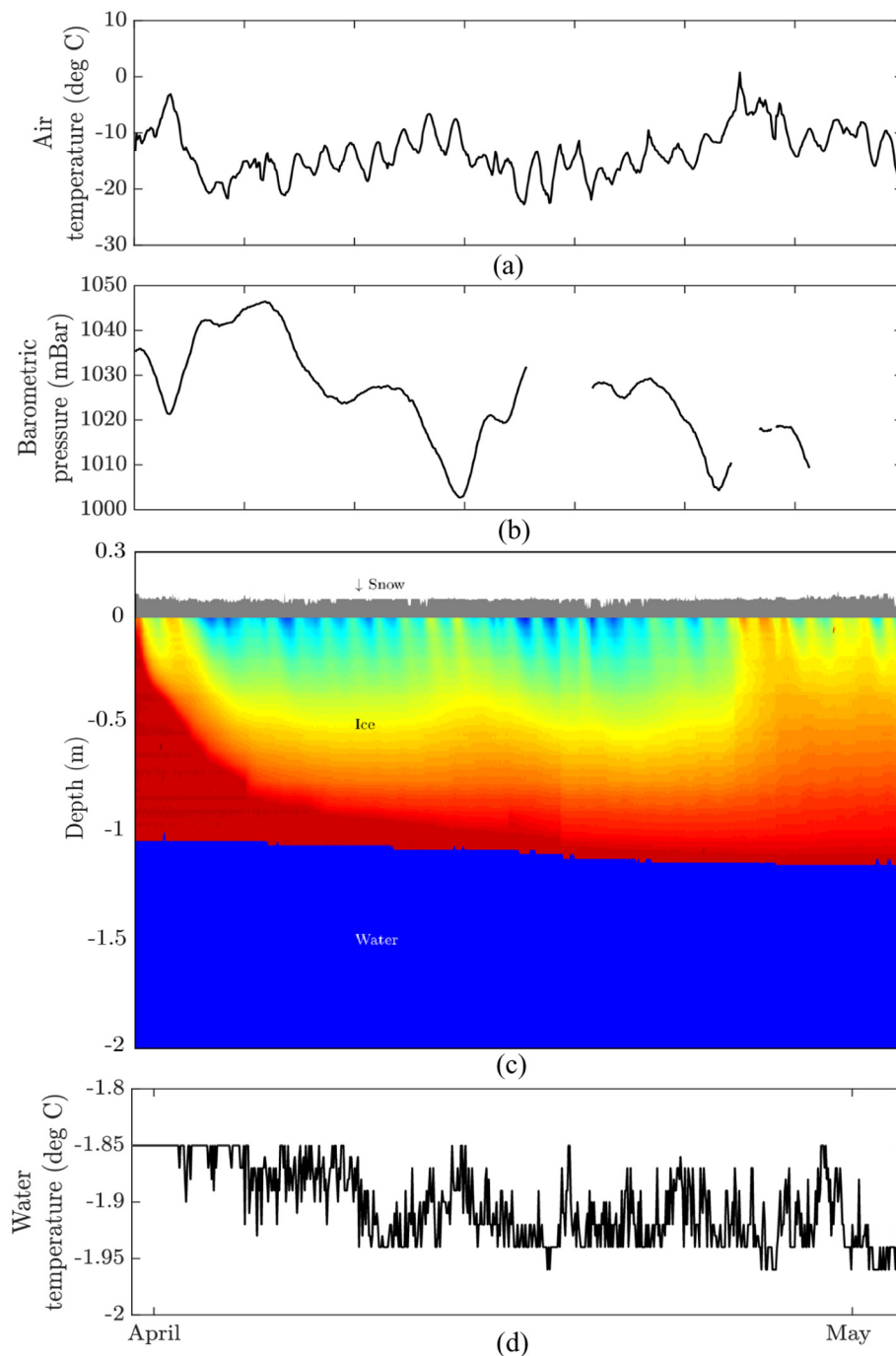

(a)   (b)

Fig. 5. (a) GPS positions of SIMB-3's deployed in the Beaufort Sea from June 2017–March 2018. (b) An SIMB-3 deployed in seasonal ice in the Beaufort Sea in March 2018 (photo courtesy of Nicholas Wright).

Fig. 6. The time series ice thickness plot of the SIMB-3 in Fig. 5 showing the buoy air temperature (a), barometric pressure (b), ice temperature, snow depth, and ice thickness (c), and water temperature (d). The thermodynamic interfaces between air and snow, snow and ice, and ice and water are easily identifiable.

onto the ice and installed in thirty minutes by a team of two people. The instrument operated for over one month, and was cut out of the ice and removed in April immediately before ice melt onset. The prototype buoy verified the ability of SIMB-3 to accomplish many of the operational design requirements, in particular, the ability to: collect the required data, be easily transported, be easily deployed and recovered, be open water stable, and be cold weather operable. Other requirements such as lifespan and durability were left to future deployment opportunities for validation.

Since June of 2017, several other SIMB-3's have been built and deployed to support a variety of scientific programs. Fig. 5,a shows the GPS locations of these buoys, and Fig. 5,b shows a picture of a deployment in March 2018.

The buoy in Fig. 5,b was deployed in seasonal ice in the Beaufort Sea during March of 2018, and corresponds to the yellow track in Fig. 5,a. Initial ice and snow thicknesses were 103.5 cm and 7.5 cm, respectively. During deployment, the buoy was assembled, stood up, and inserted into the ice through a single 25 cm drilled hole. After insertion, the buoy floated upright in the hole until freeze in, which took about 24 h. The frozen connection to the ice is maintained into the melt season through the use of a highly reflective white vinyl wrap to reduce the albedo of the SIMB-3 and prevent solar heating and melt out. Some preferential melting around SIMB-3 likely still occurs during the late melt season, but is difficult to directly observe because the instruments are almost never revisited post-deployment. When preferential melting occurs, the rangefinder readings should not be immediately influenced

because their location of measurement is 29 cm outward from the center of the buoy hull.

Data from the surface and underwater acoustic rangefinders and temperature string were combined to create a time series plot of ice thickness and temperature (Fig. 6,c). On this plot the air/snow, snow/ice, and ice/water interfaces are easily identified and the vertical temperature profile is visualized by color. Time series of air temperature, barometric pressure, and underwater temperature are plotted in Fig. 6,a,b,c. Underwater temperature was taken at the location of the underwater rangefinder, which was approximately 2.9 m below the ocean surface. Several erroneous values were removed from the barometric pressure graph (indicated by white spaces).

5. Conclusions

An improved ice mass balance buoy that is capable of autonomous operation in seasonal Arctic sea ice has been described. The instrument, referred to as SIMB-3, was comprehensively designed using input from a variety of stakeholders, ranging from the principal scientists to the deployment teams. It was engineered to be highly reliable, survivable, deployment friendly, and significantly lower-cost relative to previous Ice Mass Balance Buoys platforms. SIMB-3 uses a floating spar-type hull design and is capable of operation through the complete melting of the ice cover. The buoy directly measures snow/ice surface and bottom positions using acoustic rangefinders from a fixed reference frame above and below the ice and can distinguish between surface and bottom growth/ablation. The instrument is also equipped with a custom, low-cost, expandable datalogger that integrates the rangefinders, air temperature and pressure sensors, a high resolution vertically oriented temperature string, a GPS, and Iridium satellite communications. During test deployments, occurring from June 2017–March 2018, the platform succeeded in meeting its operational design requirements, most notably: reliable determination of local thermodynamic ice mass balance and rapid deployability. Platform development and deployments will continue as deployment results, feedback, and opportunities become available.

References

Carmack, E., Melling, H., 2011. Cryosphere: warmth from the deep. Nat. Geosci. 4, 7–8. https://doi.org/10.1038/ngeo1044.

Hauser, J.R., Griffin, A., Klein, R.L., Katz, G.M., Gaskin, S.P., 2010. Quality function deployment (QFD). In: Wiley International Encyclopedia of Marketing. American Cancer Society. https://doi.org/10.1002/9781444316568.wiem05023.

Jackson, K., Wilkinson, J., Maksym, T., Meldrum, D., Beckers, J., Haas, C., Mackenzie, D., 2013. A novel and low-cost sea ice mass balance buoy. J. Atmos. Ocean. Technol. 30, 2676–2688. https://doi.org/10.1175/JTECH-D-13-00058.1.

Kay, J.E., Gettelman, A., 2009. Cloud influence on and response to seasonal Arctic Sea ice loss. J. Geophys. Res. 114, 1–18. https://doi.org/10.1029/2009JD011773.

Krishfield, R., Proshutinsky, A., Tateyama, K., Williams, W., Carmack, E.C., Timmermans, M.-L., 2014. J. Geophys. Res. 1271–1305. https://doi.org/10.1002/2013JC008999.

Kwok, R., Cunningham, G.F., 2015. Variability of Arctic Sea Ice Thickness and Volume from CryoSat-2 Subject Areas. pp. 2008. https://doi.org/10.1098/rsta.2014.0157.

Kwok, R., Cunningham, G.F., Wensnahan, M., Rigor, I., Zwally, H.J., Yi, D., 2009. Thinning and volume loss of the Arctic Ocean sea ice cover: 2003-2008. J. Geophys. Res. 114, 2003–2008. https://doi.org/10.1029/2009JC005312.

Laxon, S.W., Giles, K.A., Ridout, A.L., Wingham, D.J., Willatt, R., Cullen, R., Kwok, R., Schweiger, A., Zhang, J., Haas, C., Hendricks, S., Krishfield, R., Kurtz, N., Farrell, S., Davidson, M., 2013. CryoSat-2 estimates of Arctic Sea ice thickness and volume. Geophys. Res. Lett. 40, 732–737. https://doi.org/10.1002/grl.50193.

Light, B., Lindsay, R., Markus, T., Polashenski, C., Jones, K.F., Laroche, D., Elder, B.C., Richter-Menge, J.A., Perovich, D.K., 2011. Arctic Sea-ice melt in 2008 and the role of solar heating. Ann. Glaciol. 52, 355–359. https://doi.org/10.3189/172756411795931714.

Lindsay, R., Schweiger, A., 2015. Arctic Sea ice thickness loss determined using subsurface, aircraft, and satellite observations. Cryosphere 9, 269–283. https://doi.org/10.5194/tc-9-269-2015.

Massonnet, F., Jahn, A., 2012. Observational Needs for Sea Ice Models Short Note. pp. 1–6.

Microchip, 2018. SAM D21 Family. [WWW Document]. URL. http://ww1.microchip.com/downloads/en/DeviceDoc/SAMD21-Family-DataSheet-DS40001882D.pdf.

Morison, J.H., Aagaard, K., Falkner, K.K., Hatakeyama, K., Moritz, R., Overland, J.E., Perovich, D., Shimada, K., Steele, M., Takizawa, T., Woodgate, R., 2002. North Pole Environmental Observatory Delivers Early Results. Eos (Washington. DC). pp. 83. https://doi.org/10.1029/2002EO000259.

Perovich, D.K., 2003. Thin and thinner: sea ice mass balance measurements during SHEBA. J. Geophys. Res. 108, 8050. https://doi.org/10.1029/2001JC001079.

Perovich, D.K., Polashenski, C., 2012. Albedo evolution of seasonal Arctic Sea ice. Geophys. Res. Lett. 39, 1–6. https://doi.org/10.1029/2012GL051432.

Perovich, D.K., Richeter-Menge, J.A., Jones, K.F., Light, B., 2008. Sunlight, water, and ice: extreme Arctic Sea ice melt during the summer of 2007. Geophys. Res. Lett. 35, 2–5. https://doi.org/10.1029/2008GL034007.

Polashenski, C., Perovich, D., Richter-Menge, J., Elder, B., 2011. Seasonal ice mass-balance buoys: adapting tools to the changing Arctic. Ann. Glaciol. 52, 18–26. https://doi.org/10.3189/172756411795931516.

Richter-Menge, J.A., Perovich, D.K., Elder, B.C., Claffey, K., Rigor, I., Ortmeyer, M., 2006. Ice mass balance buoys: a tool for measuring and attributing changes in the thickness of the Arctic Sea ice cover. Ann. Glaciol. 44, 205–210. https://doi.org/10.3189/172756406781811727.

Richter-Menge, J.A., Jeffries, M.O., Osborne, E., 2018. Arctic. Bull. Am. Meterological Soc. 143–174.

Rothrock, D.A., Percival, D.B., Wensnahan, M., 2008. The decline in arctic sea-ice thickness: separating the spatial, annual, and interannual variability in a quarter century of submarine data. J. Geophys. Res. Ocean. 113, 1–9. https://doi.org/10.1029/2007JC004252.

Stroeve, J.C., Serreze, M.C., Holland, M.M., Kay, J.E., Malanik, J., Barrett, A.P., 2012. The Arctic's rapidly shrinking sea ice cover: a research synthesis. Clim. Chang. 110, 1005–1027. https://doi.org/10.1007/s10584-011-0101-1.

Untersteiner, N., 1961. On the mass and heat budget of arctic sea ice. Arch. Met. Geoph. Biokl. A. 12, 151–182. https://doi.org/10.1007/BF02247491.